The 13-atom encapsulated gold cage clusters

Zhang Chuan-Hui(张川晖)†, Cui Hang(崔 航), and Shen Jiang(申 江)

Institute of Applied Physics, University of Science and Technology Beijing, Beijing 100083, *China*

(Received 4 May 2012; revised manuscript received 1 June 2012)

The structure and the magnetic moment of transition metal encapsulated in a Au_{12} cage cluster have been studied by using the density functional theory. The results show that all of the transition metal atoms (TMA) can embed into the Au_{12} cage and increase the stability of the clusters except Mn. Half of them have the I_h or O_h symmetry. The curves of binding energy have oscillation characteristics when the extra-nuclear electrons increase; the reason for this may be the interaction between parity changes of extra-nuclear electrons and Au atoms. The curves of highest occupied molecular orbital–lowest unoccupied molecular orbital (HOMO–LUMO) gap also have oscillation characteristics when the extra-nuclear electrons increase. The binding energies of many M@Au_{12} clusters are much larger than that of the pure Au_{13} cluster, while the gaps of some of them are less than that of Au_{13}, so maybe Cr@Au_{12}, Nb@Au_{12}, and W@Au_{12} clusters are most stable in fact. For magnetic calculations, some clusters are quenched totally, but the Au_{13} cluster has the largest magnetic moment of 5 μ_B. When the number of extra-nuclear electrons of the encapsulated TMA is even, the magnetic moment of relevant M@Au_{12} cluster is even, and so are the odd ones.

Keywords: cluster, icosahedral, cuboctahedral, fullerenes

PACS: 31.15.es, 31.10.+z, 75.90.+w **DOI:** 10.1088/1674-1056/21/10/103102

1. Introduction

In recent years, metallic clusters have attracted much attention in many fields, such as catalysis, electronics, magnetics, and optics,[1,2] due to their novel physical and chemical properties that vary with cluster size, geometric structure, and temperature.[3,4]

Clusters with particular magic numbers (13, 55, and 147) of atoms can be particularly stable. And the 13-atom case is the most studied one among these clusters. It has the first geometric closed shell for both the icosahedral (I_h) and the cuboctahedral (O_h) structures. Sakurai *et al.*[5] experimentally showed that 13 is a common magic number for many transition-metal clusters, including Fe_{13}, Ti_{13}, Zr_{13}, Nb_{13}, and Ta_{13}, but they could not provide a clear evidence for the exact atomic arrangement. Until now, it has been difficult and rare to directly probe the structures of such small clusters experimentally.

Theoretical studies and experiments of the 13-atom doped gold clusters M@Au_{12} have also been reported previously.[6−15] Ma *et al.* found that both increasing the interatomic spacing and decreasing the coordination would enhance the spin magnetic moments for the Ni_{13} cluster.[6] After the structural relaxation in the first-principles calculation, the magnetism of the Fe_{13} cluster has been found to be as strong as the bulk iron.[7] Recently, the high stability of the gold alloy fullerence M_{12}@Au_{20} (M = Na, Al, Ag, Sc, Y, La, Lu, and Au) clusters were studied by Zhang *et al.*, the results showed that their structures are like that of the icosahedral Au_{32} fullerene, and the La_{12}@Au_{20} cluster has a large binding energy and a low gap to be relatively chemically reactive.[8] Stener *et al.* calculated the icosahedral M@Au_{12} cluster (M = V, Nb, and Ta) with the density functional theory (DFT). The variation of photoabsorption spectra accorded with the nature of the encapsulated metal atom. The spin–orbit coupling played an important role in the systems.[9] Long *et al.* investigated theoretically geometric and electronic structures of 5d transition metal doped in I_h and O_h Au_{12} cages. They showed that the O_h structures are more stable for most clusters except W@Au_{12}, while the formation energy of M@Au_{12} varies with the binding energy of the metal in Au_{12}.[10] Pyykko and Runeberg theoretically predicted the stable icosahedral W@Au_{12} with a comparatively wide highest occupied molecular orbital–lowest unoccupied molecular orbital (HOMO–LUMO) gap of 3.0 eV. The unusual stability is due to the aurophilic dispersive attractions, the relativistic stabilization effects, and the magic 18-electron rule.[11] Soon after, Li *et al.* experimentally verified icosahedral and stability of W@Au_{12} and Mo@Au_{12} in the gas

†Corresponding author. E-mail: ym23_24@yahoo.com.cn

© 2012 Chinese Physical Society and IOP Publishing Ltd

phase.[12] Autschbach *et al.* did a more systemically study about the W@Au_{12} cluster by DFT.[13] Qiu *et al.* investigated M@Au_{12} clusters (M = W, Pt, Au, and Hg) by using different DFT approaches.[14] Wang *et al.* showed that the binding energies of the clusters are in the range from 2.186 eV to 7.791 eV, and large magnetic moments are observed for Cr, Fe, Co, Tc, Ru, and Rh.[15] Therefore, we will discuss some basic properties of M@Au_{12} clusters, where M stands for all the transition metal encapsulated, and verify whether I_h or O_h symmetry is the most stable structure.

2. Computational method

Structural optimizations and property calculations were performed using the DFT within the generalized gradient approximation (GGA),[16] and the exchange–correlation energy was implemented in the form of PW91. The effective core potential treatment and a double-numerical polarized basis set with unrestricted spin were chosen to carry out the electronic structure calculation. Self-consistent field[17] calculations were done with a convergence criterion of 10^{-5} Hartree (1 Hartree = 2 Ry = 27.21 eV) on the total energy. We applied the orbital occupation at 0 K (Fermi), and evaluated the on-site charge and magnetic moment using the Mulliken population analysis.[18] All of the structures were fully optimized without any symmetry constraint with convergence criteria of 0.002 Hartree/Å (1 Å = 0.1 nm) for the forces, 0.005 Å for the displacement, and 2×10^{-5} Hatree for the energy change. Computations were carried out with the DMol^3 program package.[19]

3. Structural and mechanical properties

Based on the theory and experiments, the 12-atom gold cage is suitable for single metal atom encapsulation.[6−15] In this case, we systemically investigate 13-atom doped gold clusters M@Au_{12}, where M denotes all the transition metal atoms (TMA). The cuboctahedral (O_h) and the icosahedral (I_h) structures are the attractive configurations of the 13-atom clusters. Hence we choose these two structures (see in Fig. 1) as the initial structures of M@Au_{12} clusters. All the M@Au_{12} clusters are optimized by allowing the atoms to relax freely, and the results are shown in Table 1.

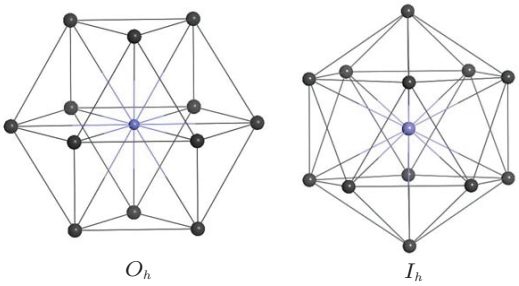


Fig. 1. (colour online) O_h and I_h structures of M@Au_{12} clusters.

From Table 1, we can see that all the TMAs can stabilize Au_{12} cages except the Mn atom. And there are few reports about the Mn-doped gold cage. We guess the reason may be that so many valencies of Mn lead to the non-uniform bonds with gold atoms. Therefore, we believe that the Mn atom is not suitable for gold cage clusters. There are some different stable structures of M@Au_{12} clusters, which are optimized starting from the O_h and the I_h configurations, such as Ti@Au_{12}, Cr@Au_{12}, Co@Au_{12}, Zn@Au_{12}, Zr@Au_{12}, Rh@Au_{12}, Ag@Au_{12}, Cd@Au_{12}, Ir@Au_{12}, and Hg@Au_{12} are O_h symmetry; while Mo@Au_{12}, Tc@Au_{12}, W@Au_{12}, and Au@Au_{12} are I_h symmetry; and the others are D_{2h}, D_{3h}, or D_{4h} symmetry. Though half M@Au_{12} clusters do not have the symmetries the same as their initial structures, they are all cage-like clusters.

For further discussion about the stability of M@Au_{12}, we calculate the binding energy E_b and the embedding energy E_e of M@Au_{12} clusters. The formulas are

$$E_\mathrm{b} = [E(M@\mathrm{Au}_{12}) - 12E(\mathrm{Au}) - E(M)]/13, \quad (1)$$

$$E_\mathrm{e} = E(M@\mathrm{Au}_{12}) - E(\mathrm{Au}_{12}) - E(M), \quad (2)$$

where E(Au) and $E(M)$ are the single atomic energies of Au atom and TMA, respectively, $E(\mathrm{Au}_{12})$ and $E(M@\mathrm{Au}_{12})$ are the lowest energies of the Au_{12} and the M@Au_{12} clusters, respectively. From Fig. 2, we can see that all the binding energies of the M@Au_{12} clusters are larger than that of the Au@Au_{12} (Au_{13}) cluster. The curves of E_b have oscillation characteristics when the extra-nuclear electrons increase, the reason may be the interaction between parity changes of extra-nuclear electron and Au atom. The binding energies of Y@Au_{12}, Ti@Au_{12}, Nb@Au_{12}, and W@Au_{12} are the largest of all. At the same time, the curves of E_e have the same trend with the curves of E_b, so we pass over the discussion.

Table 1. The symmetry (Sym.), binding energy (E_b), HOMO–LUMO gap (Gap), embedding energy (E_e), and magnetic moment (m) of M@Au_{12} clusters.

Cluster	Sym.	E_b/eV	Gap/eV	E_e/eV	m/μ_B
Sc@Au_{12}	D_{4h}	–1.483	0.12	–11.14	1
Ti@Au_{12}	O_h	–3.268	0.32	–34.34	2
V@Au_{12}	D_{2h}	–2.445	0.31	–23.64	1
Cr@Au_{12}	O_h	–2.229	1.25	-20.83	0
Mn@Au_{12}	–	–	–	–	–
Fe@Au_{12}	D_{2h}	–0.897	–0.71	–3.52	0
Co@Au_{12}	O_h	–2.585	–0.85	–25.46	3
Ni@Au_{12}	D_{4h}	–1.068	0.48	–5.74	0
Cu@Au_{12}	D_{4h}	–0.875	0.19	–3.23	1
Zn@Au_{12}	O_h	–0.762	0.88	–1.77	0
Y@Au_{12}	D_{4h}	–3.546	0.11	–37.96	1
Zr@Au_{12}	O_h	–1.444	0.15	–10.63	2
Nb@Au_{12}	D_{4h}	–3.340	0.23	–35.28	1
Mo@Au_{12}	I_h	–2.309	1.63	–21.88	0
Tc@Au_{12}	I_h	–2.521	0.11	–24.63	1
Ru@Au_{12}	D_{3d}	–0.829	0.24	–2.64	2
Rh@Au_{12}	O_h	–2.472	0.59	–24.01	3
Pd@Au_{12}	D_{4h}	–0.735	0.30	–1.41	2
Ag@Au_{12}	O_h	–0.726	0.14	–1.29	1
Cd@Au_{12}	O_h	–0.721	0.87	–1.24	0
Lu@Au_{12}	D_{4h}	–0.988	0.12	–4.70	1
Hf@Au_{12}	D_{4h}	–1.934	0.66	–17.01	0
Ta@Au_{12}	D_{4h}	–1.354	0.17	–9.46	1
W@Au_{12}	I_h	–3.228	1.80	–33.82	0
Re@Au_{12}	D_{4h}	–2.328	0.57	–22.13	1
Os@Au_{12}	D_{3h}	–0.962	0.22	–4.36	2
Ir@Au_{12}	O_h	–2.501	0.12	–24.37	1
Pt@Au_{12}	O_h	–0.977	0.78	–4.55	0
Au@Au_{12}	I_h	–0.595	0.33	–0.40	5
Hg@Au_{12}	O_h	–2.030	0.83	–18.25	0

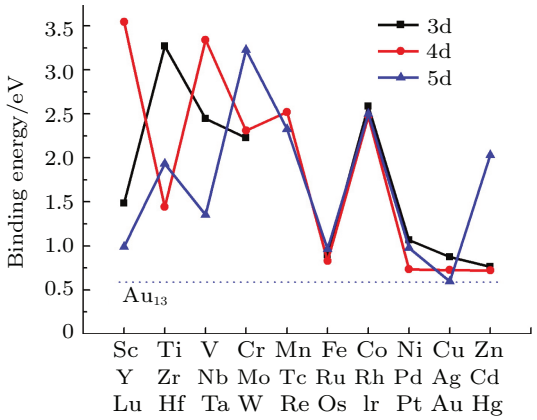


Fig. 2. (colour online) Binding energies of M@Au_{12} clusters.

Then we calculate the HOMO–LUMO gaps of M@Au_{12} clusters and show them in Fig. 3. The gap curves also have oscillation characteristics when the extra-nuclear electrons increase. As we know, the interaction of electrons will lead to the structural distortions of clusters. So the larger the HOMO–LUMO gaps of clusters, the more stable the structures. Comparing with Figs. 2 and 3, we find that the binding energies of many M@Au_{12} clusters are much larger than that of the pure Au_{13} cluster, but the gaps of some of them are less than that of Au_{13}, so maybe Cr@Au_{12}, Mo@Au_{12}, and W@Au_{12} clusters are in fact the most stable.

Magnetic properties are very important in physics. In this section, we perform a Mulliken population analysis for the magnetic moments of M@Au_{12} clusters.[18] We show the magnetic moments in Fig. 4. It is seen that the magnetic moments of Cr@Au_{12}, Fe@Au_{12}, Ni@Au_{12}, Zn@Au_{12}, Mo@Au_{12}, Cd@Au_{12}, Hf@Au_{12}, W@Au_{12}, Pt@Au_{12}, and Hg@Au_{12} clusters

are quenched totally. The Au@Au_{12} (Au_{13}) cluster has the largest magnetic moment of 5 μ_B. Similar peculiar magnetic properties also appeared in icosahedral Ni_{13} and Fe_{13} clusters.[6,7] The reason may be that the spins of electrons in the cluster formed by the same element are easy to be in the same orientation, which would lead to a large magnetic moment. An interesting phenomenon is that when the number of extra-nuclear electrons of encapsulated TMA is even, the magnetic moment of the relevant M@Au_{12} cluster is even, and so are the odd ones. The mechanism leading to this rule is still unknown. We hope that the interesting magnetic properties of M@Au_{12} clusters would be useful in spintronics in the future.

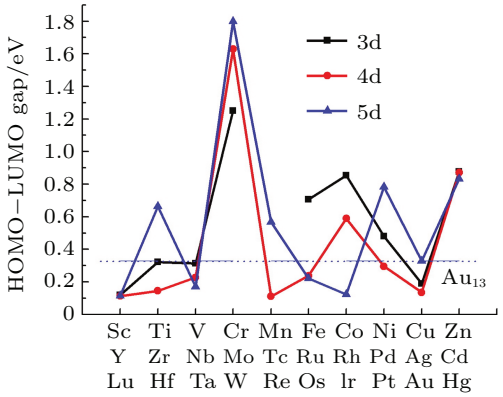


Fig. 3. (colour online) The HOMO–LUMO gaps of M@Au_{12} clusters.

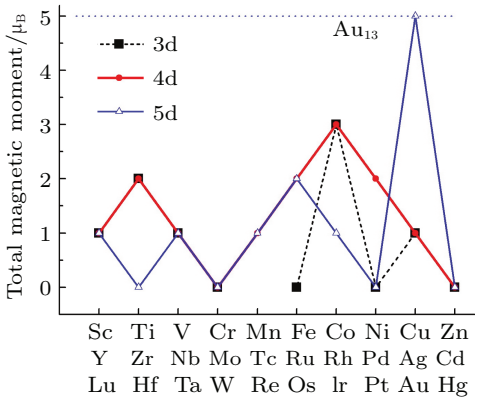


Fig. 4. (colour online) Magnetic moments of M@Au_{12} clusters. The horizontal dashed line gives the value of the Au_{13} cluster.

Charge density distributions are important for clusters, so we calculate the HOMO distributions of M@Au_{12} clusters and show the results in Fig. 5. We find that the trends of HOMO distributions of clusters with the same extra-nuclear electron configuration are similar, therefore, only the HOMO distributions of 4d electron clusters are listed for discussion. As the extra-nuclear electrons of the center atom increase, the electrons transfer from Au cage atoms to the center atom, the data get the tiptop when the d level is half-full and the s level is full (see Figs. 5(a) and 5(b)). Further increase the extra-nuclear electrons of the center atom, the electrons transfer from the center atom to Au cage atoms, the data become best when the d and the s levels are full (see Figs. 5(c) and 5(d)). The reason is that the ability of electron attraction for the center atom works on the d level mainly and works on the s level minor. So we obtain the special shapes of HOMO distributions for M@Au_{12} clusters in Fig. 5.

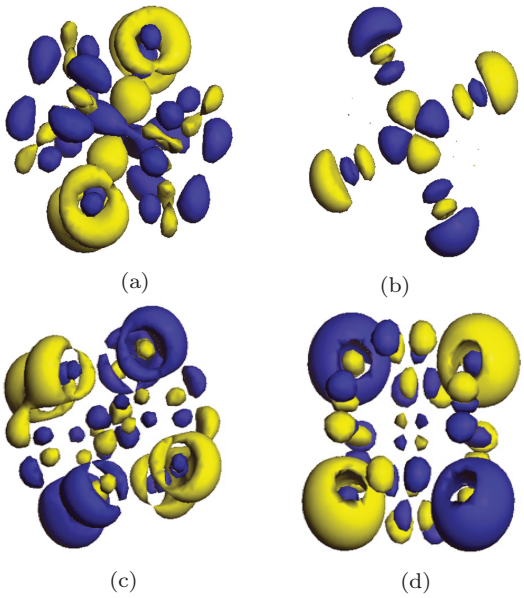


Fig. 5. (colour online) Charge density distributions of the HOMO for (a) Mo@Au_{12}, (b) Tc@Au_{12}, (c) Ag@Au_{12}, and (d) Cd@Au_{12} clusters.

And we also consider the partial densities of states (PDOS) in Fig. 6. The trends of PDOS of all the M@Au_{12} clusters with contributions from s, p, and d electrons of Au and the encapsulated atoms are the same. Therefore, only the PDOS of the M@Au_{12} clusters are listed for discussion. According to the DOS at the Fermi level, the M@Au_{12} clusters exhibit semiconductor characteristics. The overlapping sharp peaks are indicative of the interaction of encapsulated atoms and Au atoms, which leads to the orbital hybridization. The extra electron configurations are $4f^{14}5d^{10}6s^1$ for Au and half-full (full) in the d level and half-full (full) in the s level for the encapsulated atoms, but the orbital hybridization derives some new orbitals, such as d orbitals. According to the selection rules of electronic transitions, the 2p levels of Au would transit to

the 3d levels of Au or the encapsulated atoms. This is consistent with the charge transfer from Au to the encapsulated atoms.

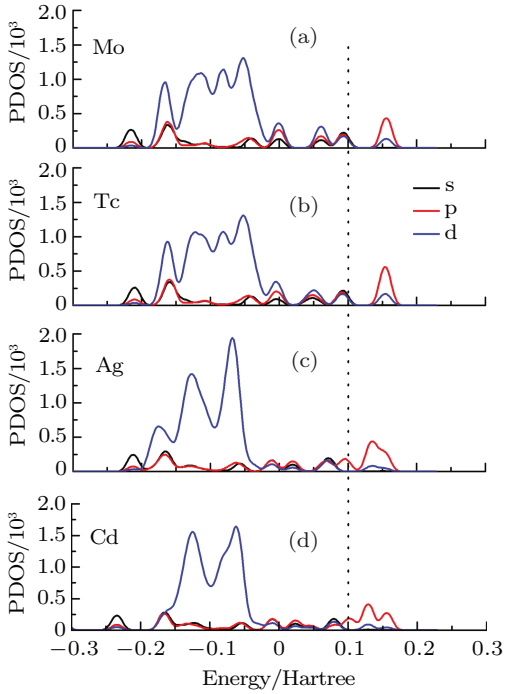


Fig. 6. (colour online) Partial densities of states of (a) Mo@Au_{12}, (b) Tc@Au_{12}, (c) Ag@Au_{12}, and (d) Cd@Au_{12} clusters.

4. Conclusion

In this paper, we investigated the structural stability and the magnetic properties of M@Au_{12} clusters by DFT calculations. The results show that all the TMA can embed into the Au_{12} cage and increase the stability of the cluster except Mn. Half of the M@Au_{12} clusters have the high symmetry of O_h or I_h structure. For magnetic calculations, some clusters are quenched totally, but the Au_{13} cluster has the largest magnetic moment of 5 μ_B. When the number of extra-nuclear electrons of the encapsulated TMA is even, the magnetic moment of the relevant M@Au_{12} cluster is even, and so are the odd ones. The electrons transfer from the Au cage atoms to the center atom, the data is best when the d level is half-full and the s level is full, and the electrons transfer from the center atom to the Au cage atoms, the data get the tiptop when the d and the s levels are full. The DOS at the Fermi level indicates that the M@Au_{12} clusters exhibit semiconductor characteristics. The overlapping sharp peaks are indicative of the interaction of encapsulated atoms and Au atoms, which leads to the orbital hybridization. We hope that these interesting properties of the M@Au_{12} clusters will be useful in nanoscience in the future.

References

[1] Aiken J D and Finke R G 1999 *J. Mol. Catal.* A: *Chem.* **145** 1
[2] Schmid G, Baumle M, Geerkens M, Heim I, Osemann C and Sawitowski T 1999 *Chem. Soc. Rev.* **28** 179
[3] Khanna S N and Castleman A W 2003 *Quantum Phenomena in Clusters and Nanostructures* (Heidelberg: Springer-Verlag)
[4] Service R F 1996 *Science* **271** 920
[5] Sakurai M, Watanabe K, Sumiyama K and Suzuki K 1999 *J. Chem. Phys.* **111** 235
[6] Ma Q M, Wang J, Li Y C, Xie Z and Liu Y 2007 *Chin. Phys.* **16** 3637
[7] Cheng Z D, Ling T and Zhu J 2010 *Chin. Phys.* B **19** 057101
[8] Zhang M, Feng X J, Zhao L X, Zhang H Y and Luo Y H 2012 *Chin. Phys.* B **21** 056102
[9] Stener M, Nardelli A and Fronzoni G 2008 *Chem. Phys. Lett.* **462** 358
[10] Long J, Qiu Y X, Chen X Y and Wang S G 2008 *J. Phys. Chem.* C **112** 12646
[11] Pyykko P and Runeberg N 2002 *Angew. Chem. Int. Ed.* **41** 2174
[12] Li X, Kiran B, Li J, Zhai H J and Wang S L 2002 *Angew. Chem. Int. Ed.* **41** 4786
[13] Autschbach J, Hess B A, Johansson M P, Neugebauer J, Patzschke M, Pyykko P, Reiher M and Sundholm D 2004 *Phys. Chem. Chem. Phys.* **6** 11
[14] Qiu Y X, Wang S G and Eugen A W H 2004 *Chem. Phys. Lett.* **397** 374
[15] Wang S Y, Yu J Z, Mizuseki H, Sun Q, Wang C Y and Kawazoe Y 2004 *Phys. Rev.* B **70** 165413
[16] Perdew J P and Wang Y 1992 *Phys. Rev.* B **45** 13244
[17] Hoheberg P C and Kohn W 1964 *Phys. Rev.* **136** 864
[18] Mulliken R S 1955 *J. Chem. Phys.* **23** 1841
[19] Delley B 1990 *J. Chem. Phys.* **92** 50